Transportation Geotechnics 38 (2023) 100876

Contents lists available at ScienceDirect

Transportation Geotechnics

journal homepage: www.elsevier.com/locate/trgeo

Use of an L-band radiometer for proximal moisture measurement in road construction

Thi Mai Nguyen *, Jeffrey P. Walker, Nan Ye, Jayantha Kodikara

Department of Civil Engineering, Monash University, Clayton, VIC 3800, Australia

ARTICLE INFO

Keywords:
Remote sensing
L-band radiometer
Soil moisture measurement
Compaction process
Typical road construction materials

ABSTRACT

The moisture content level during compaction plays a crucial role in the performance of road pavements. Current state-of-the-art methods involve manually taking small samples from a few isolated locations, making it difficult to monitor the spatial variation in moisture content along the entire construction corridor during compaction in an economically feasible manner. Therefore, finding an easy and effective method to measure soil moisture is a matter of importance. In agricultural applications, L-band passive microwave has proven to be the most accurate method for measuring soil moisture, with current satellites having a spatial resolution of approximately 40 km, which however is too coarse for road construction. Nevertheless, this technology can be deployed closer to the ground, to the point that a spatial resolution of less than 10 m is possible to achieve. Consequently, this study demonstrates the effectiveness of an L-band passive microwave radiometer for measuring soil moisture in the context of optimum compaction for road construction materials. An L-band radiometer called ELBARA-III was used to measure near-surface soil moisture in a 4.5 m × 7.5 m × 0.3 m test-bed having a sand subgrade and then an unbound granular material (UGM) sub base/base. The moisture content of the material was measured using traditional techniques such as taking thermogravimetric physical samples at targeted locations at 50 mm depth to validate the results. The results demonstrated that the L-band microwave radiometer can provide an accuracy of 5 % volumetric moisture content (VMC) or 3 % gravimetric moisture content (GMC) for sand subgrade and 2 % VMC or 1 % GMC for UGM sub base/base. An incidence angle of 0° using dual or single (horizontal or vertical) polarization was found to be the most effective configuration since it is less affected by surface roughness and is recommended for use in further field testing.

Introduction

Compaction is the process of pressing soil particles together, aimed at increasing the soil density and reducing the air volume. The main goal of this process is to achieve the desired strength properties for the soil. Accordingly, compaction plays an integral role in improving the strength and stiffness of soils in road construction [1], insufficient compaction can result in significant risks to pavement performance [2]. The degree of compaction depends on many factors including the moisture content, soil type, and compaction energy (i.e. weight of roller, number of passes). For a given compaction effort, soil densities increase and air voids decrease as moisture content increases from zero to a value known as the optimum moisture content (OMC) that gives the maximum dry density. Beyond this point, the compacted density decreases as the air is trapped by filled water voids thus keeping the particles apart. Accordingly, in order to achieve the optimum compaction, it is important to ensure compaction is performed at the optimal moisture content. Nevertheless, it is difficult to monitor the variation in moisture content during compaction along construction corridors in a cost-effective manner.

With sophisticated compaction equipment now accessible with sensors that can monitor the compaction process in real time [3], intelligent compaction (IC) has shown to be a potent technology. The majority of IC studies, however, only had limited moisture data that were collected using spot measurements [4–6]. Currently, in the field of road construction, soil moisture monitoring depends mainly on in-situ measurement techniques by manually installing sensors or taking small samples from a few isolated locations [7]. The influence area of the sensors or sample taken is relatively small with estimates limited to the area immediately adjacent to the probe/sample location. Thus, it is difficult to obtain representative soil moisture values and cannot take into account the spatial variations in the soil moisture along the

* Corresponding author.
E-mail address: thi.nguyen9@monash.edu (T.M. Nguyen).

https://doi.org/10.1016/j.trgeo.2022.100876
Received 26 July 2022; Received in revised form 27 August 2022; Accepted 29 September 2022
Available online 22 October 2022

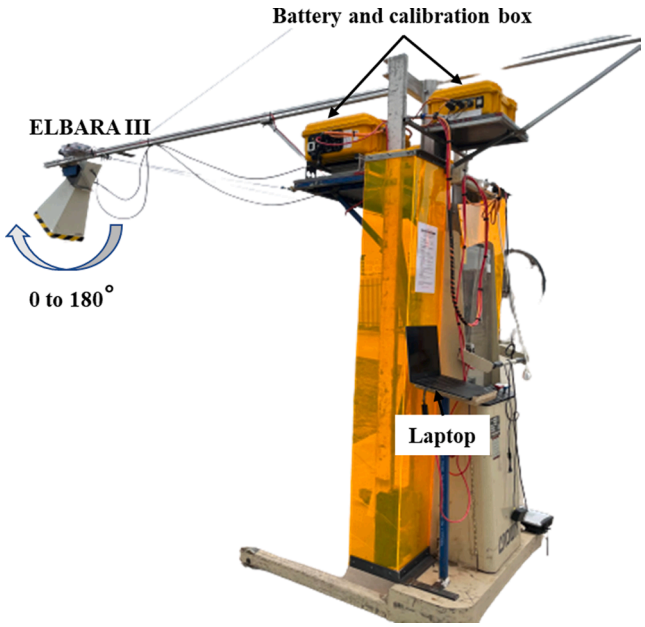

Fig. 1. The ELBARA-III system was mounted on an electronic hoist with horn antenna that could have its viewing angle changed from 0 to 180° in 5° steps.

construction corridor. Ground penetrating radar (GPR) is another non-destructive geophysical methods for soil moisture measurement [8]. The merits of this technique include high spatial resolution, low-cost, deep penetration depth, and non-destructivity [9]. However, the sensitivity to the soil texture and electrical conductivity are factors that affect the successful application of GPR [10], and it is still very manual [11]. Moreover, several GPR interpretation techniques require the presence of clearly discernible and continuous GPR reflections [8]. It follows then then that a new method for proximately monitoring the spatial variation in soil moisture during compaction along construction corridors is desirable.

It has been known for over four decades that soil moisture can be retrieved from the thermal radiance measured by an L-band radiometer [12]. In response to this understanding, the European Space Agency launched the Soil Moisture and Ocean Salinity (SMOS) mission in 2009 [13] and the National Aeronautics and Space Administration launched the Soil Moisture Active Passive (SMAP) mission in 2015 [14]. SMOS provides continuous multi-angle radiometric measurements at L-band, while SMAP incorporates a radar and a radiometer both operating at L-band and at a fixed incidence (observation) angle ($\theta = 40°$). Further, microwave radiometry at L-band (1–2 GHz) has been proven to be the most accurate and reliable method for remote soil moisture retrieval in agriculture when compared to other methods [15,16]. Using L-band, soil moisture can be measured within the top 50 mm depth [14,17]. It is therefore hypothesized that this method has the potential to provide useful soil moisture information in road construction, which has not yet been demonstrated. Although the spatial resolution provided from space is currently approximately 40 km [18], due to the technology and altitude of the satellites, there is a possibility to deploy this technology closer to the ground. Accordingly, measurements from fixed platforms, vehicles, or drones can achieve spatial resolutions less than 10 m. Radiometers mounted on towers and aircraft have been successfully used to retrieve soil moisture using L-band radiometers in several previous studies [19–23]. A drone has even been used [24–29] as well as mounting directly onto machinery [30].

There have been few agricultural studies that investigate soil moisture (SM) retrievals based on angular dependence using L-band radiometer such as discovery of SM retrieval capabilities in different multi-angular range either based on modelling [31,32] or based on observations [33,34] at variable incidence angles. The majority of the previous studies used an angle of 40° replicating the SMAP mission [30,35–37]. Zhao et al. (2020) has been discovered that with an L-band radiometer integrated into a vehicle, SM estimation algorithms operate at their best accuracy at incidence angles ranging from 40° to 45° [34]. In this study, the radiometer was set only at multi-incidence angles ranging from 30° to 65°, and it was explained that the 45° footprint fell almost in the center of the cornfield during ground measurements, which was largely unaffected by surrounding environments and heterogeneity. In turn, there were other studies [38,39] that used lowest incidence angles as a basis for their studies since the sensitivity of SM decreases with increasing incidence angle, and vegetation attenuation and the effect of surface roughness are minimized with lower incidence angles [40,41]. Miernecki et al. (2020) pointed out that most changes in observation data due to roughness effect pronounced at incidence angles >40° and a change of brightness temperature up to 8 K was observed at 60° [42]. Also found in Peischl et al. (2011) study, estimated SM results from L-band data at near-nadir views of 0-10° produced the lowest error to those obtained by ground measurement [43]. Several studies have used other approaches such as two angles and one polarization (bi-angular approach) or two polarizations and one angle (bi-polarisation approach)

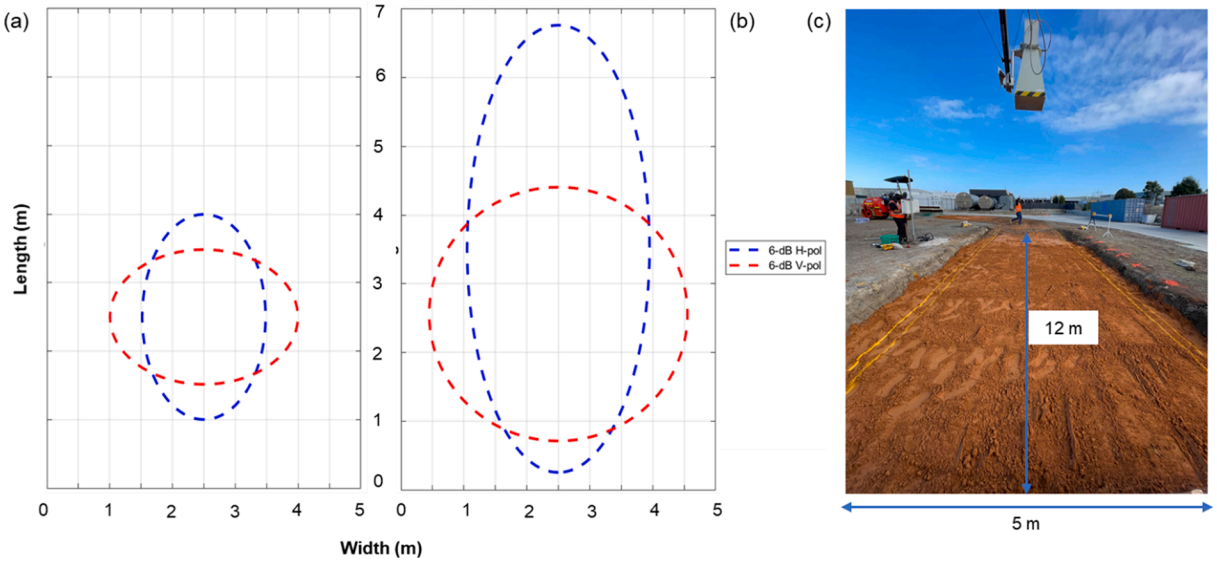

Fig. 2. ELBARA-III footprints at (a) 0°, (b) 40°, and (c) a photo of the actual sand surface corresponding to the footprints.

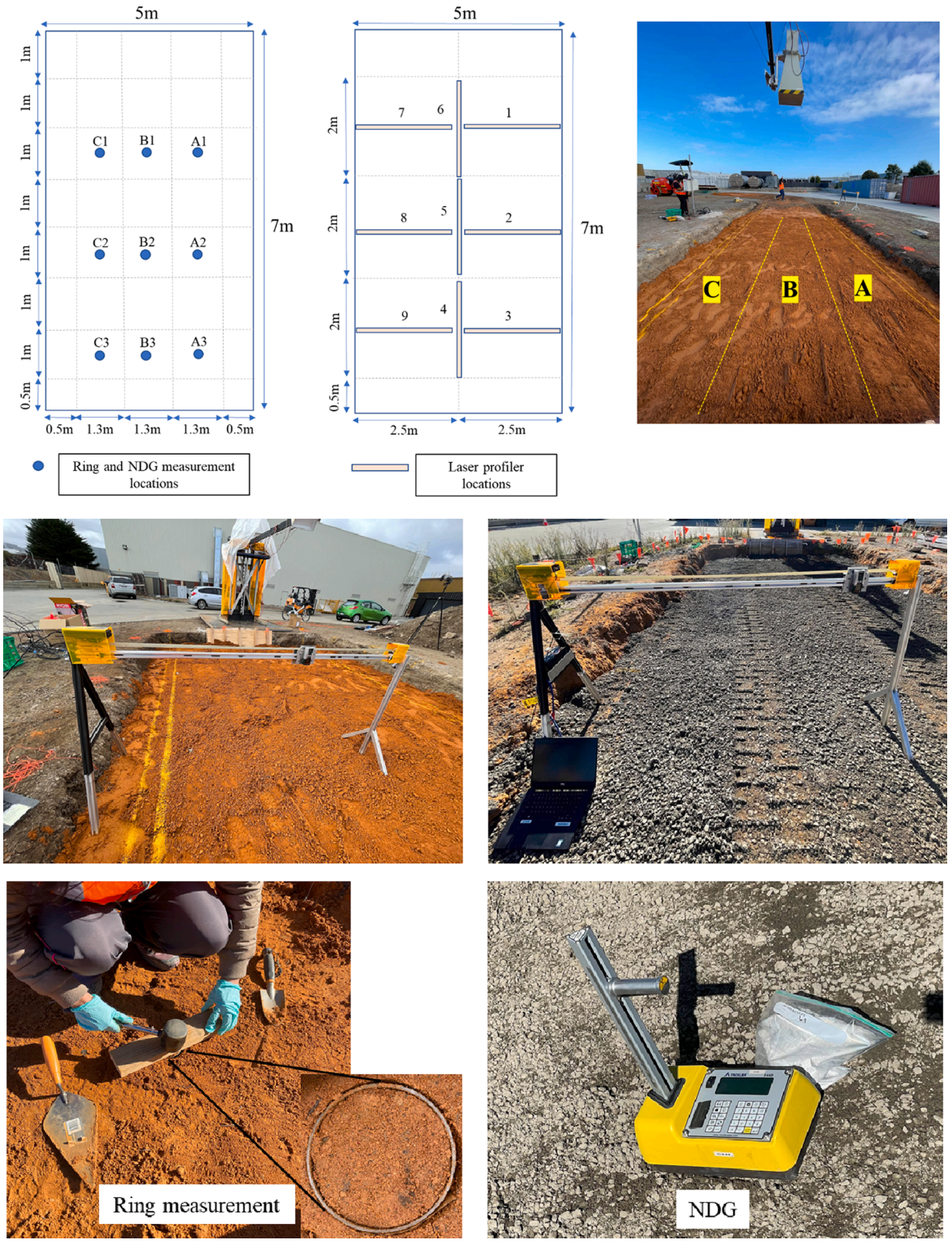

Fig. 3. The three images in the top row show the locations of 9 ring and nuclear density gauge (NDG) measurement points, the location of surface roughness measurements at 9 locations and 2 orientations, and a photo of the actual sand surface corresponding to the locations. The two images in the middle row are photos when using laser profiler to measure the surface roughness of the sand subgrade (left) and UGM sub base/base (right). The bottom row includes a photo of using the thermogravimetric ring (left) and NDG (right) to obtain moisture and density information of the sand subgrade and UGM sub base/base, respectively.

in order to improve retrieval accuracy in their results [44,45]. It can be seen that radiometric measurements or retrieval performance of SM algorithms are sensitive to the incidence angle vary with different factors including soil type, surrounding environments or the applications of the measurements. Thus, in order to find the best configuration, it is important to understand how the SM retrieval performance varies with incidence angle in specific applications.

The current methods for measuring moisture in road construction are primarily based on some points measurements at several isolated locations. The major disadvantage of these traditional methods is that they

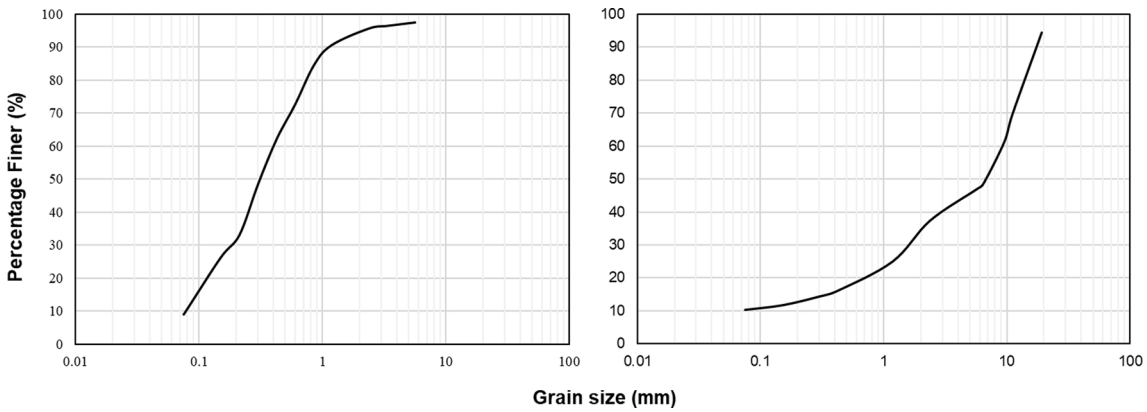

Fig. 4. Particle size distribution of sand subgrade (left) and UGM sub base/base (right) using wet sieving method.

cannot provide moisture information for the entire construction corridor. Therefore, finding a new method that can provide spatial information of soil moisture with high resolution is extremely necessary. Ideally, the higher the resolution, the more useful the information. Previous studies in the agricultural field have been carried out to provide moisture information with a high resolution of less than 10 m; in road construction applications the resolution can reach from 1 to 2 m when the radiometer is deployed close to the ground. Therefore, the main objective of this study is to explore a new method that can provide the spatial variation in soil moisture for road construction applications. Accordingly, this paper is focused on demonstrating the ability of an L-band radiometer to undertake remote moisture measurement for typical road construction materials. Additionally, it makes an assessment of the best configuration for soil moisture retrieval in this application.

Dataset

Laboratory experiments to measure soil moisture using an L-band radiometer with construction materials have been undertaken in a test-bed environment. This experiment used the L-band radiometer system commissioned by European Space Agency (ESA) [46] called ELBARA-III (ESA L-band microwave radiometer – third generation). ELBARA is an L-band radiometer with dual-polarization (vertical and horizontal polarizations) operating to measure brightness temperature (TB) within the protected frequency band 1.4–1.427 GHz, equipped with a large conical horn antenna (diameter 1.4 m, length 2.7 m, 12° full beamwidth at −3 dB). ELBARA-III (third-generation) is a portable ground-based passive microwave radiometer system with a Pickett-type horn antenna that has evolved from ELBARA-II [16] and a new internal temperature control. In this study, ELBARA-III was mounted on a movable electric host (Fig. 1), such that the horn antenna height above the ground level can be adjusted by an electric control, and the horn antenna angle changed from 0 to 180°. Hence, ELBARA-III was employed to provide information on TB at different incidence angles to the soil surface (from 0 to 40° at 5° steps).

The soil test-bed was sized (5 m width × 12 m length) so as to contain the radiometer footprint as shown in Fig. 2. Compaction was carried out using a 4.5-tonne double drum roller for two test-layers of material each 150 mm thick, giving a total compacted thickness of 300 mm. Accordingly, compaction tests were performed on different materials and moisture contents. Additionally, the following equipments were used to collect corresponding ancillary and/or validation data required for this experiment (Fig. 3):

i A laser profiler was used to measure the surface roughness at 9 locations, providing several 3 m long profiles with 2 orientations.
ii A total of 12 Stevens HydraProbe soil moisture sensors were used to record vertical soil temperature and soil moisture profiles in 50 mm depth increments at two locations. Two temperature sensors were used to record the soil surface temperature at two locations. Measurements were made at two-minute sampling steps for understanding temporal variation.
iii The thermogravimetric ring (for sand subgrade) and Nuclear Density Gauge (NDG) (for Unbound Granular Material (UGM) sub base/base) methods were used to measure the top 50 mm soil moisture and density variation across the footprint at 9 locations.
iv Soil texture analysis was conducted for each material to obtain the required parameters for the dielectric mixing model used by the soil moisture retrieval algorithm.

In this experiment, a sand material was first used because i) it is a commonly used subbase/subgrade material; ii) it is readily available in Melbourne; and iii) the existing dielectric mixing models are directly applicable to this material. The second material was an Unbound Granular Material (UGM) sub base/base, which is a continuously graded granular material, predominantly consisting of crushed rock particles [47]. UGM sub base/base was used because i) it is a typical base or subbase material used in road construction; and ii) it is readily available from the supplier. Wet sieving method was performed to obtain information on the particle size distribution (>0.75 μm) for two materials (Fig. 4). X-ray diffraction (XRD) method was used to analyse the size distribution to obtain the proportion of clay in each sample. Details of the two soil materials including optimum moisture content and sand and clay fraction are presented in Table 1.

Two sets of experiments were performed at different levels of compaction and different soil moisture contents, being a sand subgrade and UGM sub base/base, respectively. The material was first homogenised using a concrete batching plant and then compacted in two layers (each 150 mm thick). Before and after compacting the material, the ELBARA-III was employed to measure the soil brightness temperature (TB) at different angles, followed by the ancillary measurements. Further, the moisture content of the soil was measured using traditional techniques at targeted locations to validate the results. Upon completion, the material was removed and changed to another material, and the same process repeated. More detail on the experimental setup is presented in Table 2.

Six sets of experiments were performed for the sand subgrade, each with two layers of compacted soil at different moisture contents. The first layer was compacted on 29-Jul, 14-Sep 2021, and 1-Feb 2022, while the second layer was on 30-Jul, 16-Sep 2021 and 02-Feb 2022. Thus, there are six lots of experimental data prior to compaction and six lots of experimental data after completing compaction.

Four sets of experiments were also performed for the UGM sub base/base, each with two layers of compacted UGM sub base/base at different moisture contents. The first layer was compacted on 04-Feb and 10-Feb 2022 while the second layer was on 07-Feb and 11-Feb 2022,

Fig. 5. The compaction process consisted of evenly spreading the transported material to the test-bed using a bobcat, levelling the surface and conducting compaction with a roller for sand subgrade (from left to right, top to middle). The procedures for UGM sub base/base were similar and are shown in the two images at the bottom.

Table 1
Soil materials and its optimum moisture contents and texture information were used in the experiments.

Materials	Optimum moisture contents – OMC % (GMC)	Gravel (%)	Sand (%)	Silt (%)	Clay (%)
Sand subgrade	OMC = ~12 %	2.96	88	8.11	0.93
UGM sub base/base	OMC = ~4.5 %	55.66	34	8.89	1.45

Table 2
Steps taken in the experiment.

Step	Task (Fig. 5)
1	The material was prepared to the desired moisture content, this work has been done by the supplier.
2	Transport and spread the material into the test-bed using a bobcat - first layer
3	Measure: ● SM and temperature profile using Steven HydraProbes: insert 6 Steven Hydra-Probes into the soil layer at 2 locations with 5 cm depth increments (3 sensors each location), ● TB using ELBARA-III at different angles (0–40° at 5° steps), ● Surface roughness using laser profiler at 9 locations, ● Surface SM and density at 9 locations using ring thermogravimetric (for sand subgrade) and NDG (for UGM (sub base/base) methods.
4	Compact the soil to a thickness of around 150 mm using a roller.
5	Repeat step 3.
6	Fill the material into the test-bed for the second layer and repeat steps 3–5.
7	Remove compacted material, change to another material, and repeat steps 1–6.

respectively. Thus, there are four lots of experimental data prior to compaction and four lots of experimental data after completing compaction.

The moisture content was carried out from dry to wet condition. Details of the SM content including gravimetric moisture content (GMC) and volumetric moisture content (VCM), dry density and their standard deviation (STD) in each of the experiments for sand subgrade and UGM sub base/base are shown in Table 3, with photos of the setup of these experiments in Fig. 6. The STD determined from 9 point-based traditional measurements on the test-bed in order to display the variation of moisture and density data.

Methodology

Theory of Passive Microwave Emission Model

The distinct contrast between the dielectric properties of liquid water (~80; depending on temperature, electrolyte solution, and frequency) and dry soil (<4) makes the soil dielectric permittivity highly sensitive to soil water content variation. Microwave sensors can therefore detect the change of the dielectric constant of the water-soil mixture because of increased moisture [48].

Smooth bare soil surface

For a smooth bare soil, the microwave energy emission (i.e. the microwave brightness temperature; *TB*) that is observed by a radiometer can be expressed as the product of the soil physical temperature and the surface emissivity. For soil moisture retrieval applications at low altitudes, the temperature contributed from the atmosphere or the sky can be ignored ($TB_{sky} = \sim 4$ K [49,50]). Therefore, the brightness temperature of a bare soil surface is related to the physical temperature of the soil (T_{soil}) through the soil emissivity such that.

$$TB = eT_{soil} = (1 - r)T_{soil}, \tag{1}$$

where r is the smooth surface reflectivity and e is the soil emissivity, which depend on the soil dielectric constant [51].

The surface emissivity is typically expressed in terms of the surface reflectivity described by the Fresnel equation for horizontally (H) and vertically polarized waves (V) by.

$$r_H(\theta) = \left(\frac{cos\theta - \sqrt{\varepsilon_s - sin^2\theta}}{cos\theta + \sqrt{\varepsilon_s - sin^2\theta}}\right)^2, \tag{2}$$

$$r_V(\theta) = \left(\frac{\varepsilon_s cos\theta - \sqrt{\varepsilon_s - sin^2\theta}}{\varepsilon_s cos\theta + \sqrt{\varepsilon_s - sin^2\theta}}\right)^2, \tag{3}$$

where ε_s is the soil relative dielectric constant at a given frequency, which can be expressed by water content in soil via a dielectric mixing model, and θ is the incidence angle relative to nadir (an angle measurement with the downward vertical is zero). Consequently, for a smooth bare soil surface, the reflectivity, and thus the brightness temperature (*TB*), depends on three input variations: the dielectric constant, the incidence angle and the radiation polarization.

Table 3
Details of testing time, soil moisture content, dry density and their standard deviation (STD) in each experiment lot for sand subgrade and UGM sub base/base.

Sand subgrade	**Before compaction**						**After compaction**					
	Gravimetric moisture content - GMC (%)	**STD (%)**	**Volumetric moisture content - GMC (%)**	**STD (%)**	**Dry density (g/cm^3)**	**STD (g/cm^3)**	**Gravimetric moisture content - GMC (%)**	**STD (%)**	**Volumetric moisture content - GMC (%)**	**STD (%)**	**Dry density (g/cm^3)**	**STD (g/cm^3)**
29-Jul (compact first layer)	11	0.5	19	0.2	1.53	0.08	10	0.8	22	2	1.92	0.05
30-Jul (compact second layer)	11	0.7	19	1	1.54	0.07	10	1.7	21	4.1	1.83	0.06
14-Sep (compact first layer)	12	0.5	20	2.3	1.38	0.12	12	0.5	23	1	1.75	0.02
16-Sep (compact second layer)	12	0.3	19	0.7	1.43	0.09	12	0.5	23	1.9	1.79	0.06
01-Feb (compact first layer)	6	0.6	8	1.3	1.2	0.1	6	0.2	13	1.2	1.89	0.11
02-Feb (compact second layer)	7	0.4	10	0.6	1.31	0.07	7	0.4	12	0.9	1.78	0.1
UGM sub base/base	**Before compaction**						**After compaction**					
	Gravimetric moisture content - GMC (%)	**STD (%)**	**Volumetric moisture content - GMC (%)**	**STD (%)**	**Dry density (g/cm^3)**	**STD (g/cm^3)**	**Gravimetric moisture content - GMC (%)**	**STD (%)**	**Volumetric moisture content - GMC (%)**	**STD (%)**	**Dry density (g/cm^3)**	**STD (g/cm^3)**
04-Feb (compact first layer)	3.4	0.4	6.1	0.7	1.75	0.06	3.3	0.2	6.9	0.5	2	0.04
07-Feb (compact second layer)	3.2	0.3	5.5	0.7	1.67	0.05	3.1	0.2	6.02	0.7	1.97	0.12
10-Feb (compact first layer)	5.5	0.3	10.3	0.7	1.75	0.07	4.8	0.3	10.7	0.7	2.14	0.1
11-Feb (compact second layer)	4.6	0.4	8.9	0.9	1.86	0.04	3.7	0.2	8.3	0.6	2.19	0.05

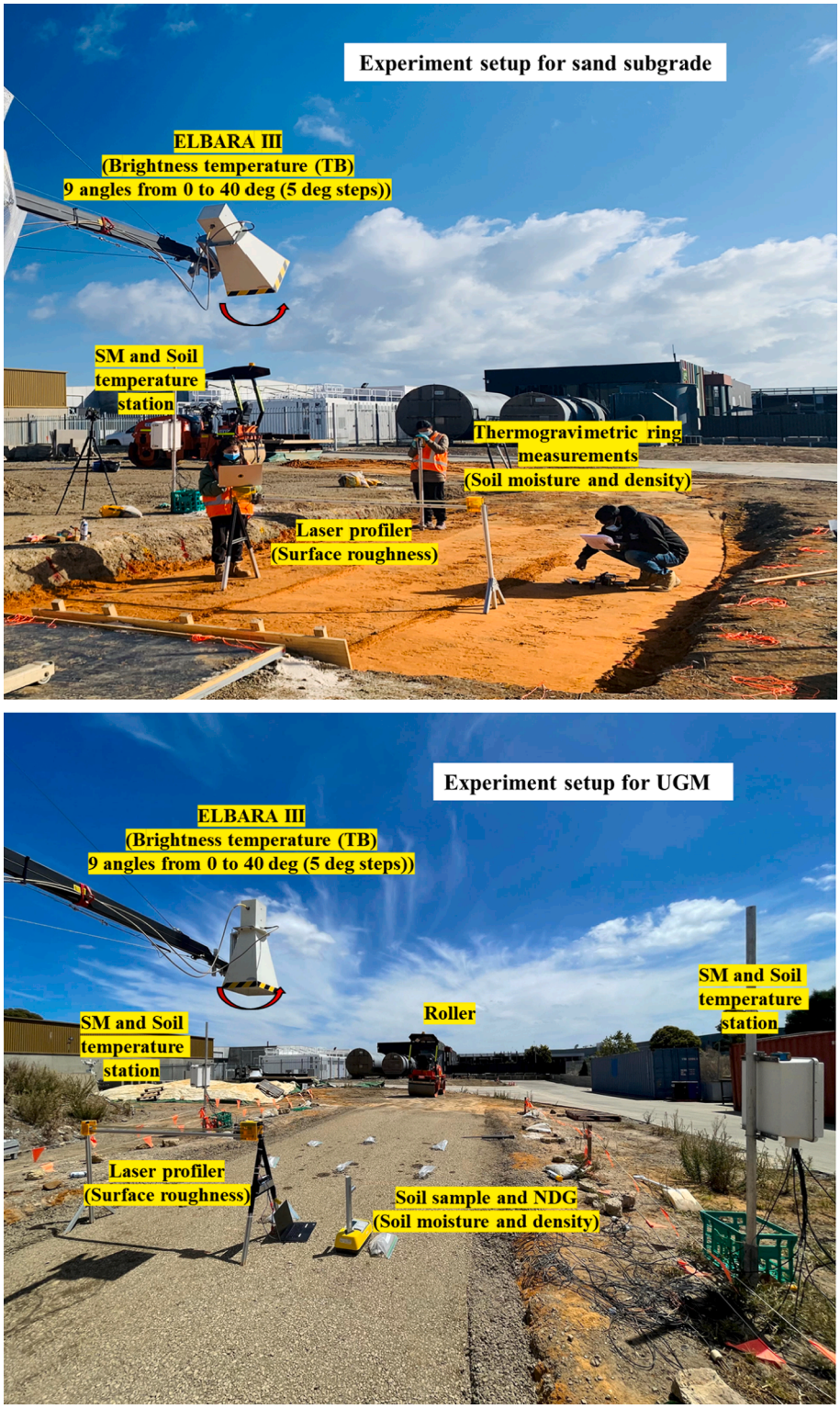

Fig. 6. Experiment set up in this study for sand subgrade (top) and UGM sub base/base (bottom).

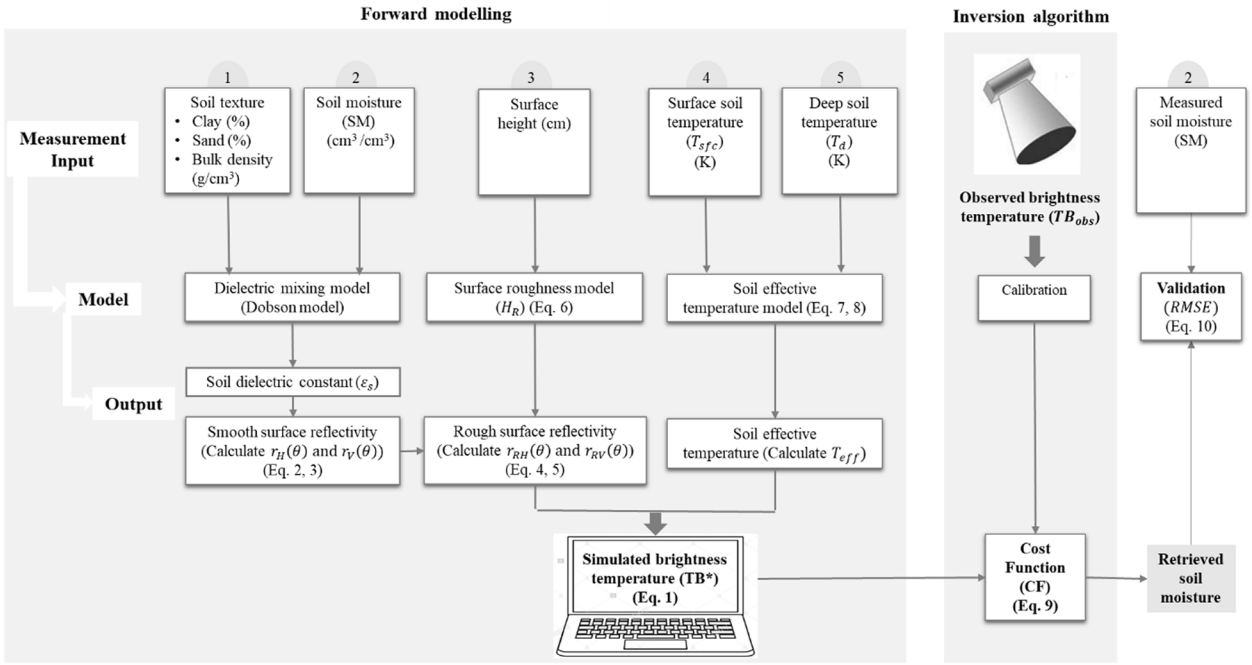

Fig. 7. Process of the soil moisture retrieval model.

Dielectric mixing model

The dielectric constant is a complex number that describes the propagation of an electromagnetic wave through a material. It consists of a real part that shows a material's ability to polarize in response to the electric field against free space, and an imaginary part that denotes a medium's ability to absorb waves [40]. There are several factors that can affect the soil dielectric value such as soil texture, temperature, salinity, and electromagnetic wavelength.

In the soil moisture retrieval model, dielectric constant values can be used as an output or an input depending on the model and its use in the forward or reverse mode. A dielectric mixing model is therefore required to convert between dielectric constant and volumetric soil moisture. Several soil dielectric models have been developed, including empirical [52], semi-empirical [53], and physical [54,55] models. The Dobson dielectric mixing model [53] was used in this study. This model was developed based on experiments using five soil samples to compute the soil dielectric constant in the microwave spectrum of 1.4–18 GHz. The Dobson model required input data including the volumetric soil moisture, soil effective temperature, clay and sand fraction, and soil bulk density [56].

Correction procedures for deviation from smooth bare soil

Impact of surface roughness

Generally, natural land surfaces have soil surfaces that are rough rather than smooth, typically resulting in a greater level of emission. Consequently, compensation is required for rough surfaces, with the sensitivity of the microwave signal to soil moisture being reduced as the surface roughness increases [57,58]. Thus, a general semi-empirical equation has been proposed that describes the effect of surface roughness on the microwave emission based on two best-fit parameters Q_R and H_R [59], and defines the H_R parameter dependent on the incidence angle and polarisation [33] such that.

$$r_{RH}(\theta) = ((1 - Q_R(\theta))r_H(\theta) + Q_R(\theta)r_V)e^{\left(-H_{RH}cos^{N_{RH}}(\theta)\right)}, \quad (4)$$

$$r_{RV}(\theta) = ((1 - Q_R(\theta))r_V(\theta) + Q_R(\theta)r_H)e^{\left(-H_{RV}cos^{N_{RV}}(\theta)\right)}, \quad (5)$$

where r_{RH} and r_{RV} are the rough surface reflectivity for horizontal (H) and vertical polarizations (V), r is the smooth soil reflectivity, Q_R is a polarisation mixing parameter, H_R is a surface roughness parameter. While H_R is calculated from the standard deviation of surface heights, the Q_R depends on the electromagnetic frequency and its value is very small at the L-band range [60], and set equal to 0 in many publications [57,58]. N_R in the exponential term is the angular dependence. Based on long term measurements, a subsequent study found that $N_R \approx 1$ at horizontal and $N_R \approx -1$ at vertical polarisation over a relatively smooth soil [61].

Parameterization for the model roughness parameter H_R has been proposed with a dependence on the Standard Deviation of the surface height (SD), given by Choudhury et al. (1979) [62].

$$H_R = (2k^*SD)^2, \quad (6)$$

where k is the wavenumber expressed as $k = 2\pi/\lambda$, and λ is the wavelength.

Impact of vertical soil moisture and temperature profiles on effective temperature

It can be seen from Eq. (1) that the observed microwave emissions depend on both soil moisture and temperature, under an assumption that they are constant over the sensing depth. In the microwave region, the top few centimeters of soil have a major impact on microwave emission at low frequencies [63], and typically these layers have considerable variation. Consequently, assumptions for the homogeneity of moisture and temperature in the vertical distribution of the soil are not satisfied for estimating the TB and emissivity of most soil surfaces. To account for this variability, the observed TB is normalized by an effective radiance temperature of the soil, with a simple linear parameterisation given by Choudhury et al. (1982) [64].

$$T_{eff} = T_d + C(T_{sfc} - T_d), \quad (7)$$

where T_{sfc} is the observed surface temperature (0–50 mm), T_d is the deep soil temperature (500 or 1000 mm), and C is an empirically-defined weighting function. The C parameter is based on relative contributions of the individual layers to the surface microwave radiation.

Table 4
Summary table of parameters measured and used in the moisture retrieval model in each experiment lot for sand subgrade and UGM sub base/base.

Sand subgrade			Soil surface temperature - T_{sfc} (K)	Soil deep temperature - T_d (K)	Standard Deviation of the surface height (cm)	Volumetric moisture content - VMC (%)	Bulk density (g/cm^3)	Sand fraction (%)	Clay fraction (%)
First layer	29-Jul	Before compaction	284.57	283.05	1.16	19	1.7	88	0.93
		After compaction	285.65	285.15	0.94	22	2.12		
	14-Sep	Before compaction	287.27	286.02	1.45	20	1.55		
		After compaction	292.96	286.25	0.93	23	1.96		
	01-Feb	Before compaction	294.95	294.12	1.86	8	1.3		
		After compaction	295.87	295.45	1.02	13	2		
Second layer	30-Jul	Before compaction	282.67	282.8	1.11	19	1.71		
		After compaction	284.07	283.07	1.19	21	2.02		
	16-Sep	Before compaction	288.43	285.85	1.12	19	1.6		
		After compaction	294.3	286.33	1.02	23	2		
	02-Feb	Before compaction	294.35	291.75	1.67	10	1.4		
		After compaction	295.38	294.94	1.02	12	1.9		
UGM sub base/base			**Soil surface temperature - T_{sfc} (K)**	**Soil deep temperature - T_d (K)**	**Standard Deviation of the surface height (cm)**	**Volumetric moisture content - VMC (%)**	**Bulk density (g/cm^3)**	**Sand fraction (%)**	**Clay fraction (%)**
First layer	04-Feb	Before compaction	291.89	291.15	1	6.1	1.81	34	1.45
		After compaction	304.31	295.22	0.89	6.9	2.08		
	10-Feb	Before compaction	296.3	295.96	0.87	10.3	1.83		
		After compaction	300.01	297.74	0.74	10.7	2.24		
Second layer	07-Feb	Before compaction	297.84	295.73	0.7	5.5	1.72		
		After compaction	313.75	297.72	0.67	6.2	2.03		
	11-Feb	Before compaction	294.62	292.38	0.82	8.9	1.95		
		After compaction	303.12	295.55	0.48	8.3	2.27		

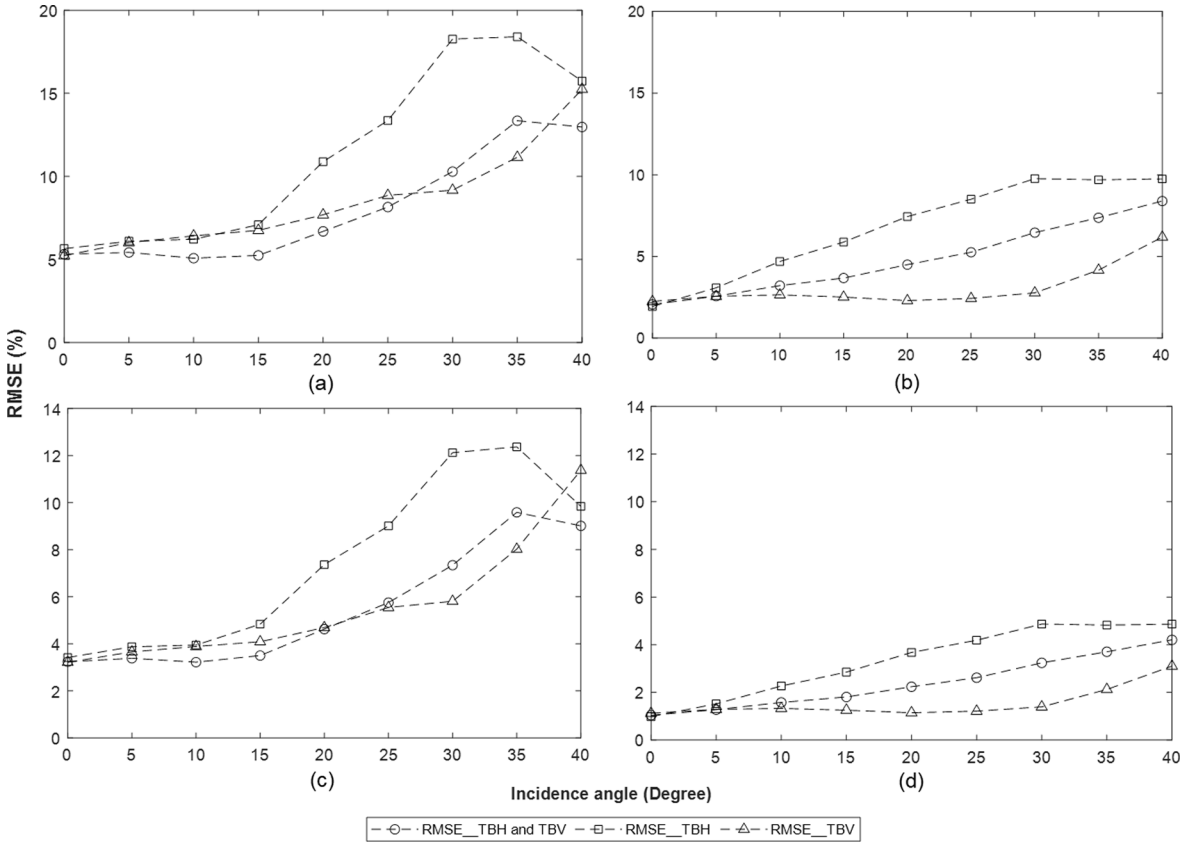

Fig. 8. RMSE of soil moisture retrieval (single angle) results at incidence angles from 0 to 40° for all experiments before and after the compaction process for sand subgrades (figures (a) and (c)) and for UGM sub base/base (figures (b) and (d)). Figures (a) and (b) show the results in terms of volumetric moisture content (VMC) while figures (c) and (d) are in terms of gravimetric moisture content (GMC).

Therefore, it determines the contribution ratio of the deep and surface layers to the effective soil temperature. A slightly improved formula has been proposed by Wigneron et al. (2001) [58] to account for the dependence of C on soil moisture.

$$C = (SM/w_0)^{b0}, \tag{8}$$

where C is a function of soil moisture SM (m^3/m^3) in the top 0–30 mm of the soil. The w_0 (m^3/m^3) and b_0 are semi-empirical parameters depending on the soil properties. Parameters $w_0 = 0.398$ and $b_0 = 0.181$

Table 5
Number of cases in each incidence angle combination.

Number of angles	1 angle	2 angles	3 angles	4 angles	5 angles	6 angles	7 angles	8 angles	9 angles
Number of combinations	9	36	84	126	126	84	36	9	1

were calibrated by Wigneron et al. (2008) [65]. In this application, soil deep temperature data collected from Stevens HydraProbe soil moisture sensors and soil surface temperature data collected from temperature sensors were used as inputs for the retrieval model.

Inversion algorithm to retrieve soil moisture

ELBARA-III was used to provide observed TB (TB_{obs}) from the soil surface at different incidence angles, a laser profiler provided the roughness information, and Stevens HydraProbe soil moisture sensors and temperature sensors were used to obtain the vertical distribution of the soil temperature. These parameters together with soil texture, bulk density information, and a first guess of soil moisture were used as input to the forward model to predict the soil surface TB (TB^*). The best estimate of soil moisture was then inverted using an iterative method [66] to minimize a cost function (CF) calculated from the differences between observed (TB_{obs}) and simulated TB (TB^*) as.

$$CF = \frac{\sum (TB_{obs} - TB^*)^2}{\sigma(TB)^2}, \quad (9)$$

where the sum of the difference between TB_{obs} and TB^* was calculated using both polarizations and all available incidence angles; $\sigma(TB)$ is the standard deviation related to the TB_{obs}, which was set to 1 K in this study. 1 K represents the variability of the observed TB data in the experiments.

In summary, the observed TB from ELBARA-III were used together with ancillary measurements (surface roughness, soil temperature, soil density, and soil texture information) to retrieve the volumetric moisture content of the compacted soil and then converted to gravimetric moisture content based on the density. Further, the moisture content of the soil was measured using the traditional technique at targeted locations to validate results from the model. Specifically, a forward model for bare soil was established using Eqs. (1) to (8). The dielectric model by Dobson was adopted for the sand subgrade and UGM sub base/base. Accordingly, the forward simulation predicted the TB using soil surface parameters, soil temperature, and surface roughness information together with an assumed soil moisture, and the soil moisture retrieved by iteratively running the forward model to match with the known TB observed from ELBARA-III according to the cost function in Eq. (9). Based on both the simulation and the retrieval, gravimetric and volumetric SM was determined and compared with soil moisture

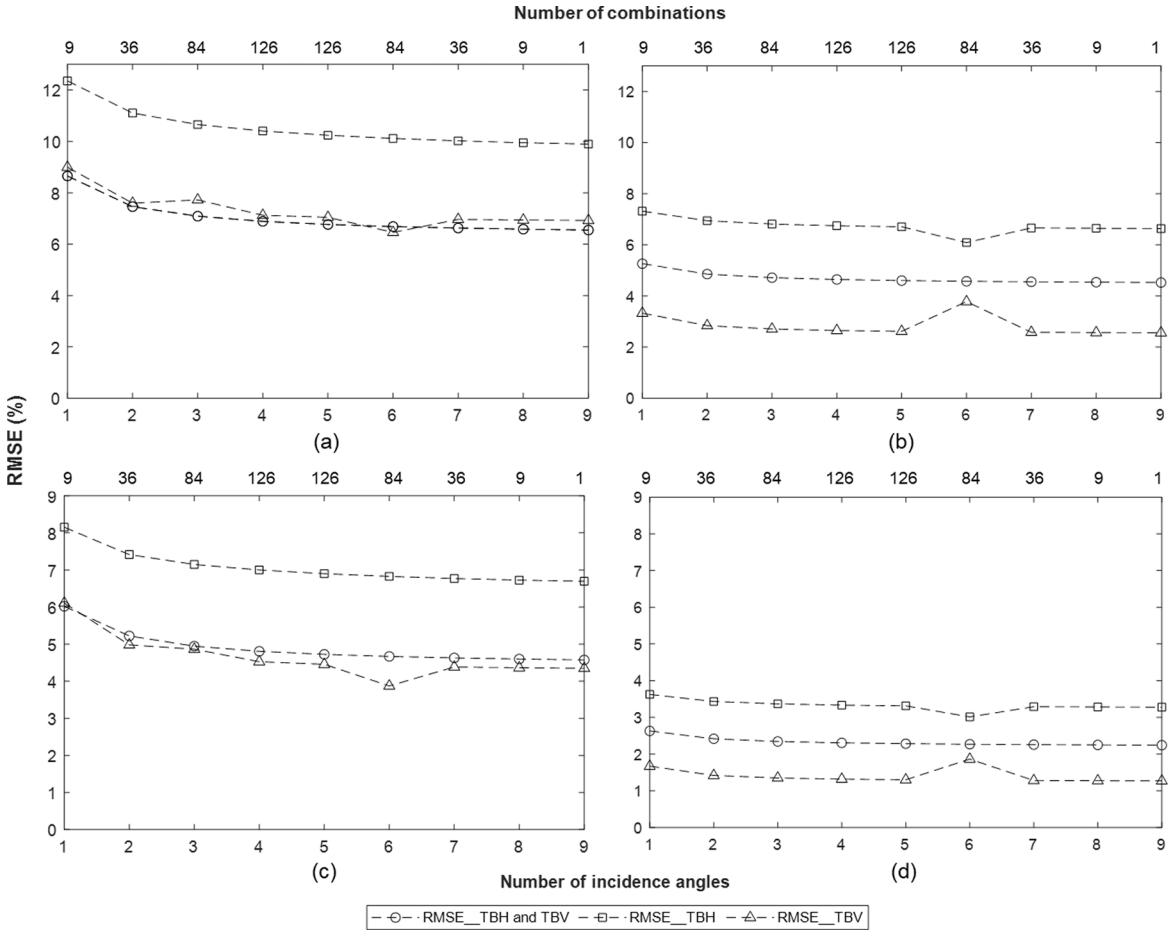

Fig. 9. RMSE of soil moisture retrieval results at different combinations of incidence angles (from 1 to 9 angles) for all experiments including before and after compaction when using a single (horizontal or vertical) or dual (horizontal and vertical) polarizations for sand subgrade (figures (a) and (c)) and for UGM sub base/base (figures (b) and (d)). Figures (a) and (b) show the results in terms of volumetric moisture content (VMC) while figures (c) and (d) are in terms of gravimetric moisture content (GMC).

measurement from the traditional technique. The sequence of these steps can be found at Fig. 7. The parameters measured for use in the moisture retrieval model for each experiment lot are shown in Table 4.

RMSE was calculated to determine the accuracy of the retrieval model as.

$$RMSE = \left(\frac{1}{n}\sum (SM_{est} - SM_{mea})^2\right)^{0.5}, \quad (10)$$

where SM_{mea} was the average of measured soil water content from the traditional technique at targeted locations, SM_{est} was soil water content estimated from the retrieval model, and n was the number of the experiments.

Multiple angle measurements (each 5°) can provide more input to the model. For example, from TB information at two angle observations, the model will have two inputs that include information at each of horizontal (H) and vertical (V) polarisation. Therefore, finding the appropriate number of inputs from angular measurements was performed in preparation for field application. Accordingly, different approaches to retrieve soil moisture, such as using single (horizontal or vertical) or dual (horizontal and vertical) polarizations and using a single or multi-combination incidence angle, were investigated and their results were compared for establishing the most suitable configuration for use in a vehicle setup to be used in the field.

Result

Soil moisture retrieval at a single angle

The SM was retrieved using a single (horizontal or vertical) and dual (horizontal and vertical) polarization for individual incidence angles for all sets of experiments, including those before and after the compaction process, for sand subgrade and UGM sub base/base. In comparison to using horizontal polarization, dual polarization or vertical polarization was found to be more accurate based on the RMSE results for the sand subgrade (Fig. 8 (a) and (c)), resulting in accuracy approximately 5 % VMC or 3 % GMC for incidence angles ranging from 0 to 15°. However, from 20° and upwards the accuracy gradually decreases and reaches as low as 13 % VMC or 10 % GMC at 35°. For the UGM sub base/base, the SM retrieval accuracy when using vertical polarization has been shown to provide better accuracy than using dual or horizontal polarization (Fig. 8 (b) and (d)). In general, most incidence angles resulted in a high accuracy of approximately 2 % VMC or 1 % GMC; only the results at 35 and 40° were as low as 4 and 5 % VMC or 2 and 3 % GMC, respectively. Additionally, the results showed that independent of whether dual or single (horizontal or vertical) polarization retrieval was used, the highest accuracy was always at 0° incidence angle for both materials. This result can be explained by the fact that in road construction context, where the soil surface is affected by the compaction process, leading to a

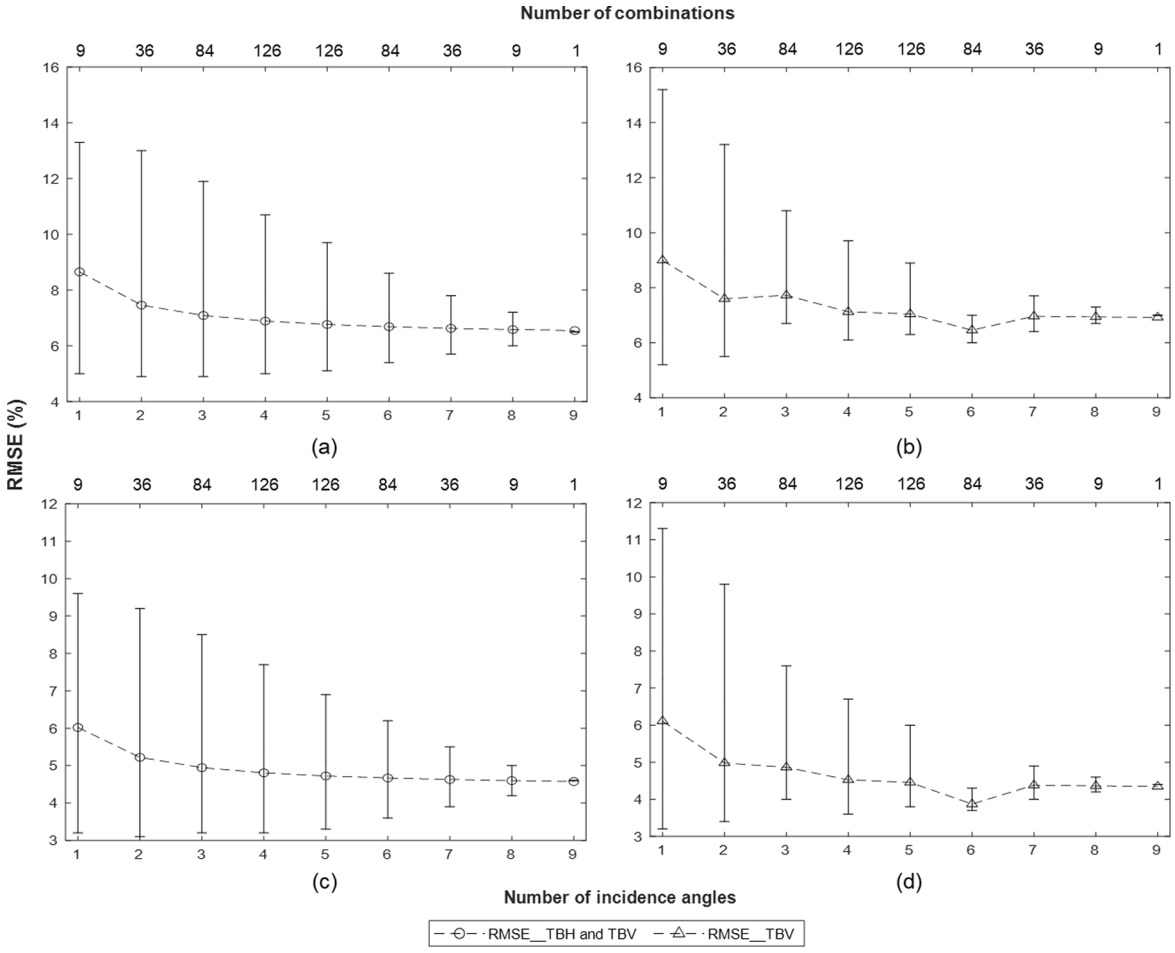

Fig. 10. The RMSE of soil moisture retrieval results when using dual (figures (a) and (c)) and vertical (figures (b) and (d)) polarization at different incidence angle combinations (from 1 to 9 angles). The whiskers represent the RMSE of the best and worst configuration result for the sand subgrade. Figures (a) and (b) show the results in terms of volumetric moisture content (VMC) while figures (c) and (d) are in terms of gravimetric moisture content (GMC).

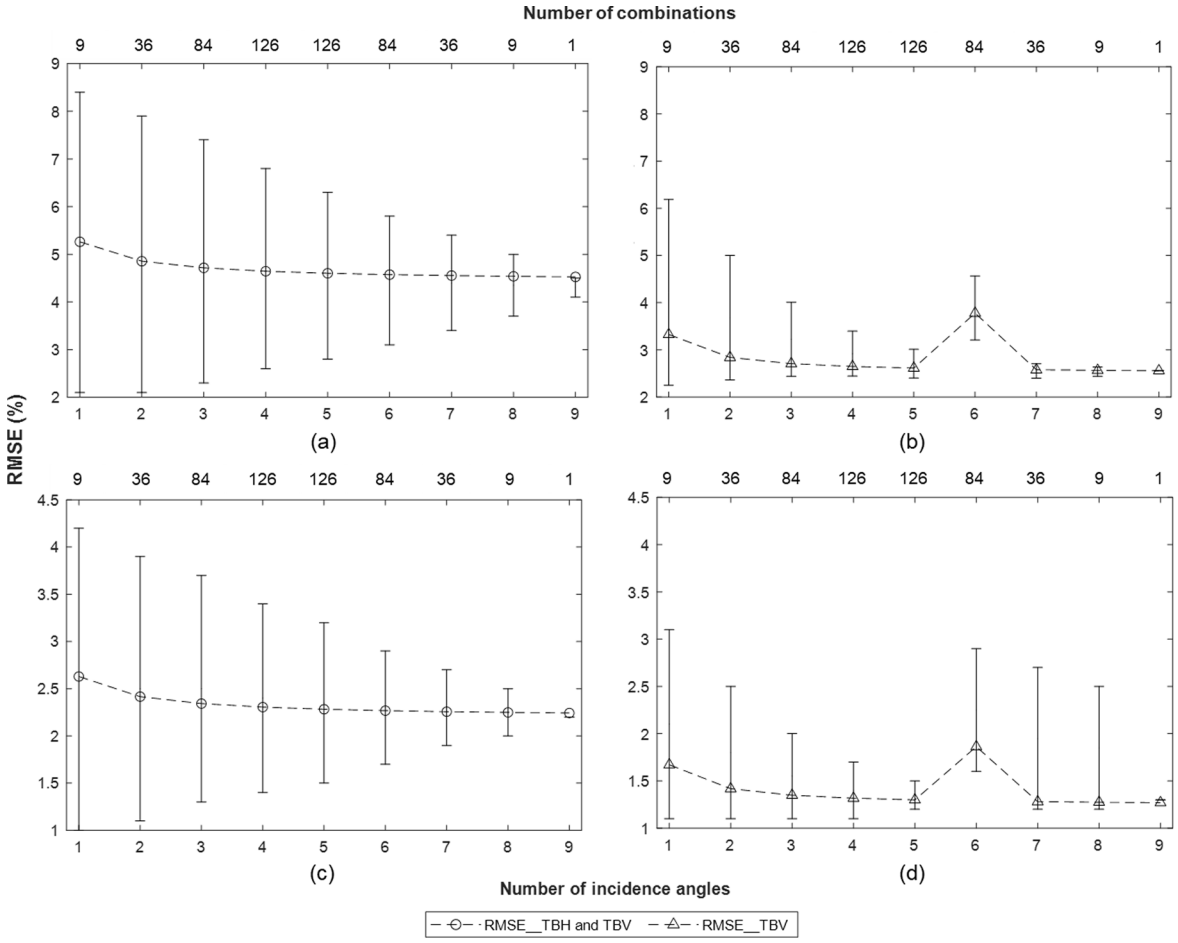

Fig. 11. As for Fig. 10 but for the UGM sub base/base.

substantial change in surface roughness before and after compacting the soil, and the roughness varies continuously between each experiment. Hence, the use of smaller incidence angles minimizes the impact of surface roughness in each measurement, resulting in the best overall SM retrieval results at 0°. Meanwhile, the observations operate at incidence angles of 35 and 40◦, respectively, are more exposed to the surface roughness effects.

Soil moisture retrieval at different angle combinations

This section explored whether using more than one incidence angle could improve the SM retrieval results. First, all cases of different incidence angle combinations are shown in Table 5. Different approaches to retrieve soil moisture, including use of single (horizontal or vertical) or dual (horizontal and vertical) polarizations, were performed to compare the results. Similar to the results when using only a single incidence angle for the sand subgrade, the results of using dual or vertical polarization gave better accuracy (RMSE $<$ 8 % VMC or 5 % GMC) than using horizontal polarization (RMSE $>$ 10 % VMC or 7 % GMC) when combining different angles (Fig. 9 (a) and (c)). In comparison with the use of dual and horizontal polarization, the use of vertical polarization led to a substantial improvement in accuracy when combining incidence angles for UGM sub base/base (RMSE $<$ 3 % VMC or 1.5 % GMC, except the combination of using 6 angles) (Fig. 9 (b) and (d)). Accordingly, only soil moisture retrieval results using both polarizations (horizontal and vertical) and vertical polarization were performed in the subsequent sections analysis.

The best and worst configuration results are presented in Figs. 10 and 11 together with the mean result for each number of incidence angle combinations, indicating that when more than one incidence angle was used for soil moisture retrieval on average the accuracy was slightly improved when choosing an angle combination at random, with the accuracy increasing as the number of angles used increased for the sand subgrade, while remaining almost unchanged for the UGM sub base/base.

The best and worst configurations for each combination are shown in Figs. 12 and 13. For the best configuration, it can be seen that the accuracy of all the combinations was almost the same (RMSE = 5 % VMC or 3 % GMC) for the sand subgrade when using dual or vertical polarization (Fig. 12). In addition, using only one incidence angle (at 10° for dual and 0° for vertical polarization) or the combination of two angles (0 and 15° for dual and 0 and 5° for vertical polarization) gave the highest accuracy when compared to the results of combining more angles. Similar results were found for the UGM sub base/base, using only one incidence (at 0°) or a combination of two angles (0 and 5° for dual and 0 and 25° for vertical polarization), resulting in a highly accurate retrieval result (RMSE = 2 % VMC or 1 % GMC) (Fig. 13).

Overall, the combination of the lowest incidence angle at 0° with another angle from 5 to 15° yielded the highest accuracy found in both materials (Figs. 14 and 15). The maximum difference of the RMSE results of these combinations is only 0.004 % VMC or 0.002 % GMC when using vertical polarization for sand subgrade (Fig. 14) and when using dual polarization for UGM sub base/base (Fig. 15). In addition, the random combination of other angles in this range (from 5 to 15°) also gives high accuracy for SM retrieval results.

For the worst configuration of sand subgrade, the accuracy reached as low as 13 % VMC or 9 % GMC when using only one incidence angle (at 35° for dual or 40° for vertical polarization) or the combination of these

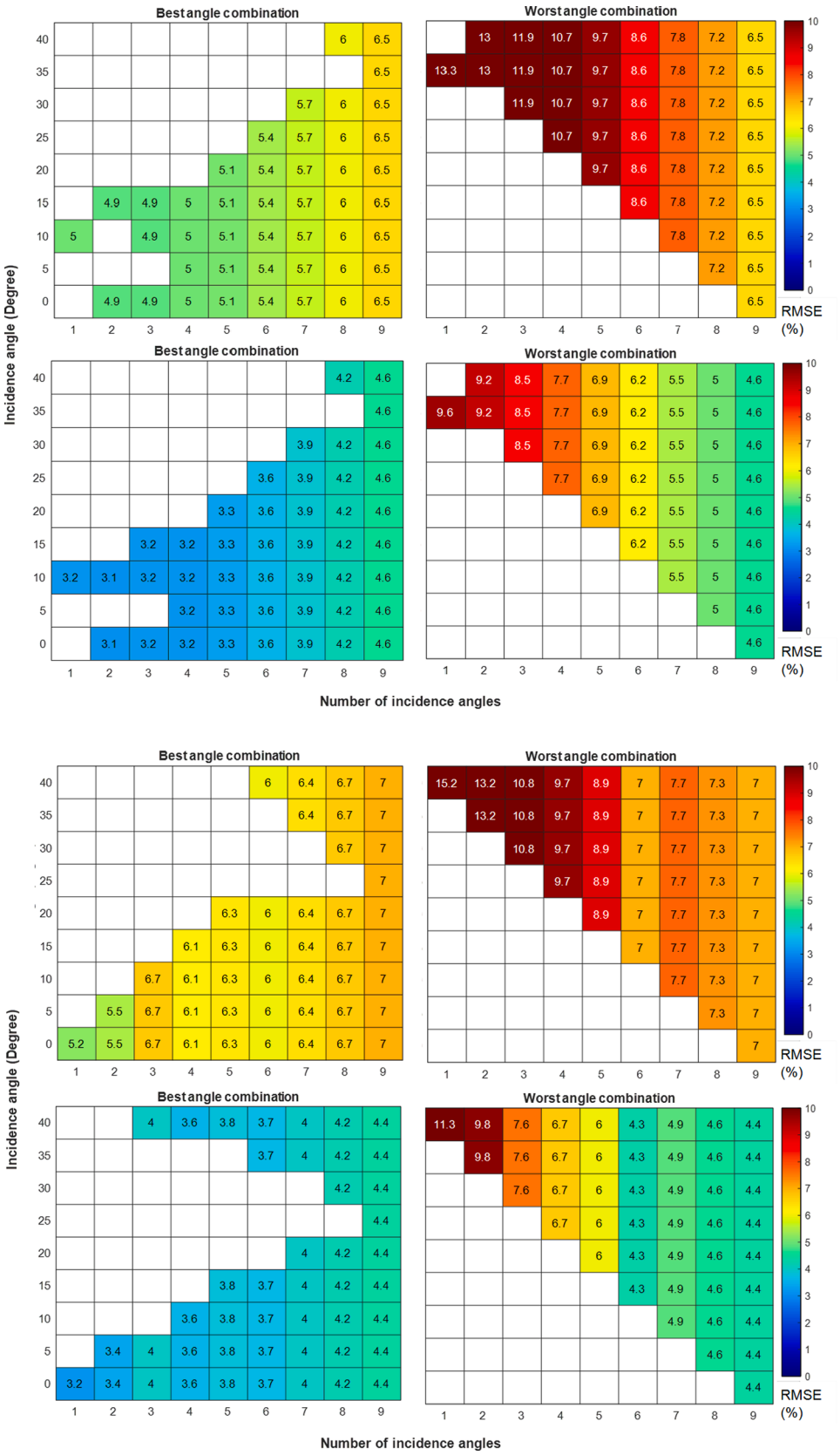

Fig. 12. The best and worst configuration of angle combination results for all experiments before and after the compaction process when using dual (4 figures at the top) and vertical (4 figures at the bottom) polarizations to retrieve SM for the sand subgrade. Each coloured square represents the angles used at each combination with the colour representing the RMSE results. In each set of figures, the top figures show the results in terms of volumetric moisture content (VMC) while the bottom is in terms of gravimetric moisture content (GMC).

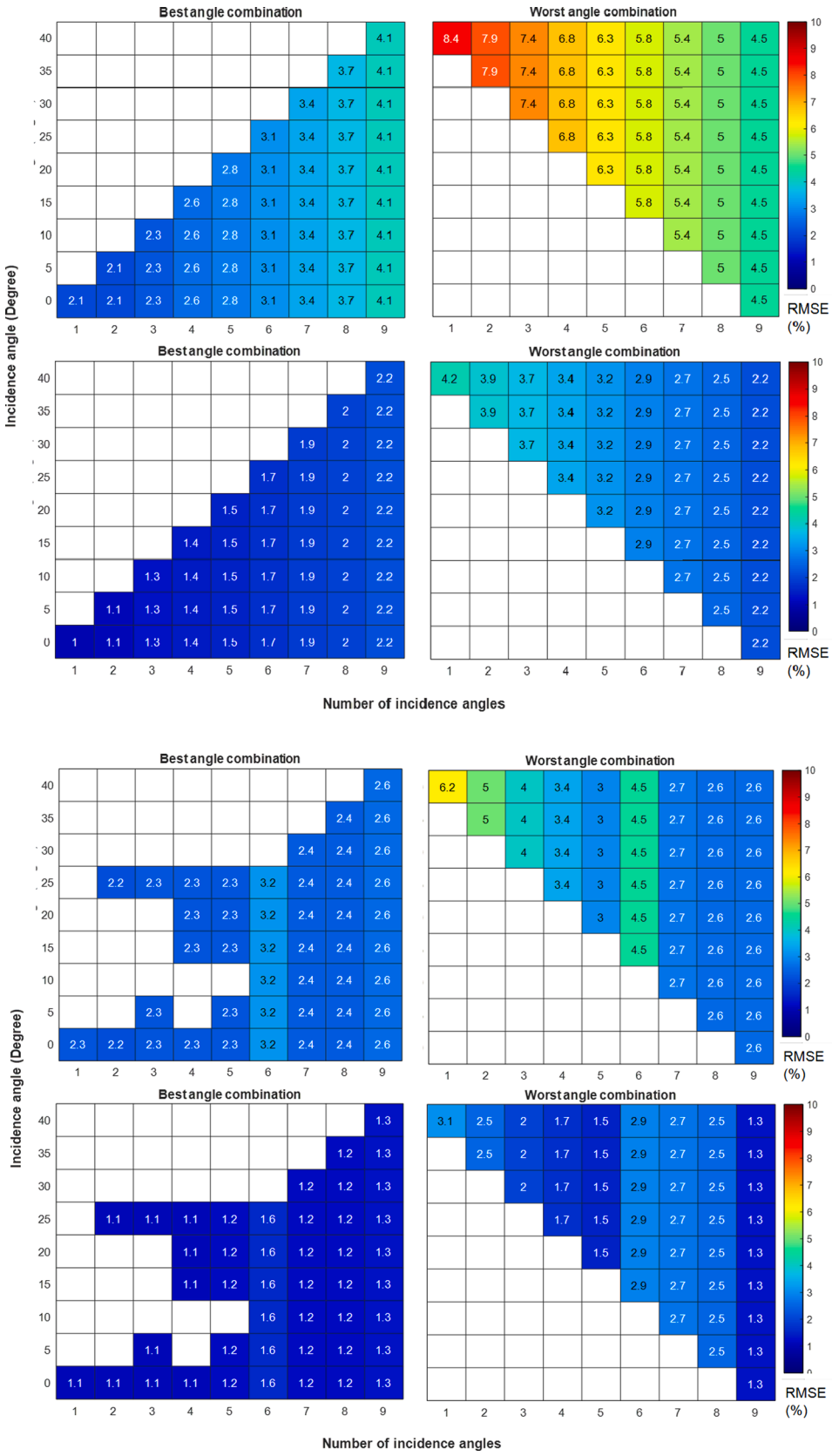

Fig. 13. As for Fig. 12 but for the UGM sub base/base.

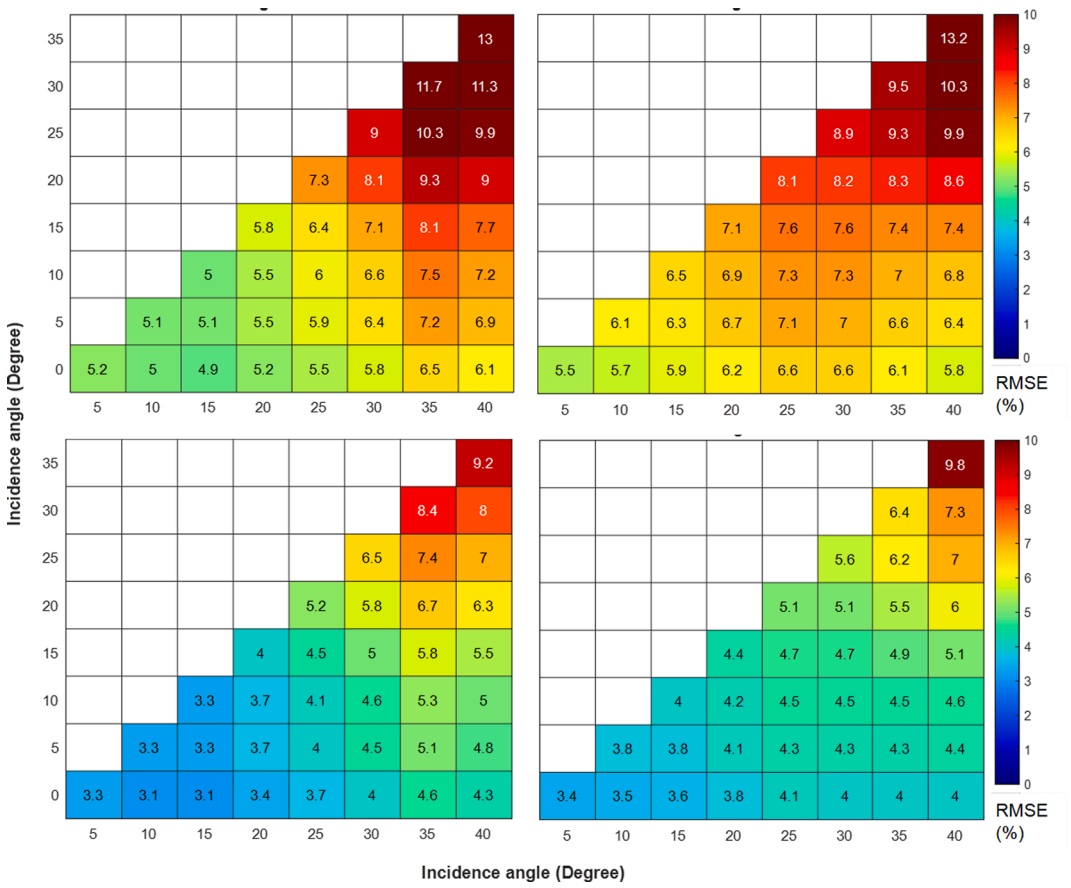

Fig. 14. The RMSE results of using 2 incidence angles for all experiments before and after the compaction process when using dual (left) and vertical (right) polarization to retrieve SM for the sand subgrade. Each coloured square represents the angles used with the colour representing the RMSE results. The top figures show the results in terms of volumetric moisture content (VMC) while the bottom is in terms of gravimetric moisture content (GMC).

two angles, and the inclusion of 35 and 40° angles in all cases (Fig. 12). Similar results are shown in Fig. 13 for UGM sub base/base with an accuracy of 8 % VMC or 4 % GMC) when using dual polarization at 40° or combining 35 and 40°, whereas it is 6 % VMC or 3 % GMC at 40° and 5 % VMC or 2.5 % GMC when combining 35° and 40° by using vertical polarization.

It can be seen that using only one incidence angle or the combination of two incidence angles is capable of providing the best retrieval results with an accuracy of 5 % VMC or 3 % GMC) for sand subgrade and 2 % VMC or 1 % GMC) for UGM sub base/base. The presence of the smaller incidence angles (i.e. 0, 5 or 10°) provides the highest accuracy while 35 and 40° or combination of these two angles caused the greatest errors for the retrieval results in every combination strategy, this result can also be explained as the effect of surface roughness becomes more evident at larger incidence angles.

Discussion

The results of this paper have demonstrated the ability of using an L-band radiometer for soil moisture retrieval for typical road construction materials. Specifically, the retrieval results achieved a very high accuracy of 2 % VMC or 1 % GMC for the UGM sub base/base and 5 % VMC or 3 % GMC for the sand subgrade material. It has been found that moisture retrieval accuracy is higher with smaller incidence angles (at 0°) and there is greater error with larger incidence angles (35 and 40°). It is appropriate to point out that this result is consistent with findings from previous studies, which could be explained by the fact that roughness is an important factor and its large variations in compaction process affects the L-band emission which is significantly reduced with smaller incidence angles.

The L-band radiometer from the space has been proven to provide up to 4 % VMC accuracy in soil moisture retrieval in agricultural applications, which means that the retrieval results for sand subgrade can potentially be further improved. Furthermore, previous studies have explored multi-parameter retrieval (i.e. SM and surface roughness or SM and soil temperature) based on different incidence angle combinations as a means of reducing the number of ancillary data requirements such as surface roughness and/or soil temperature measurement. As a result, the combined use of incidence angles suggested in this study is important for further multi-parameter retrieval studies. Further studies on this approach will be undertaken to address the problem of field data collection in road construction, where ancillary data are more difficult to obtain.

In order to retrieve soil moisture information in road construction application, once all the required input data for the retrieval model (brightness temperature from L-band radiometer, surface roughness, soil surface and deep temperature, sand and clay fraction, and bulk density) has been acquired, the interpretation of data can be completed in a short amount of time. In this study, the robustness of the retrieval algorithm has also been demonstrated by the model's capacity to retrieve moisture information for a range of data sets and materials. The findings in this paper are the first step toward deciding an optimal configuration for mounting a radiometer on a utility vehicle. Practical experiments along the construction corridor (several kilometers long) are scheduled to be

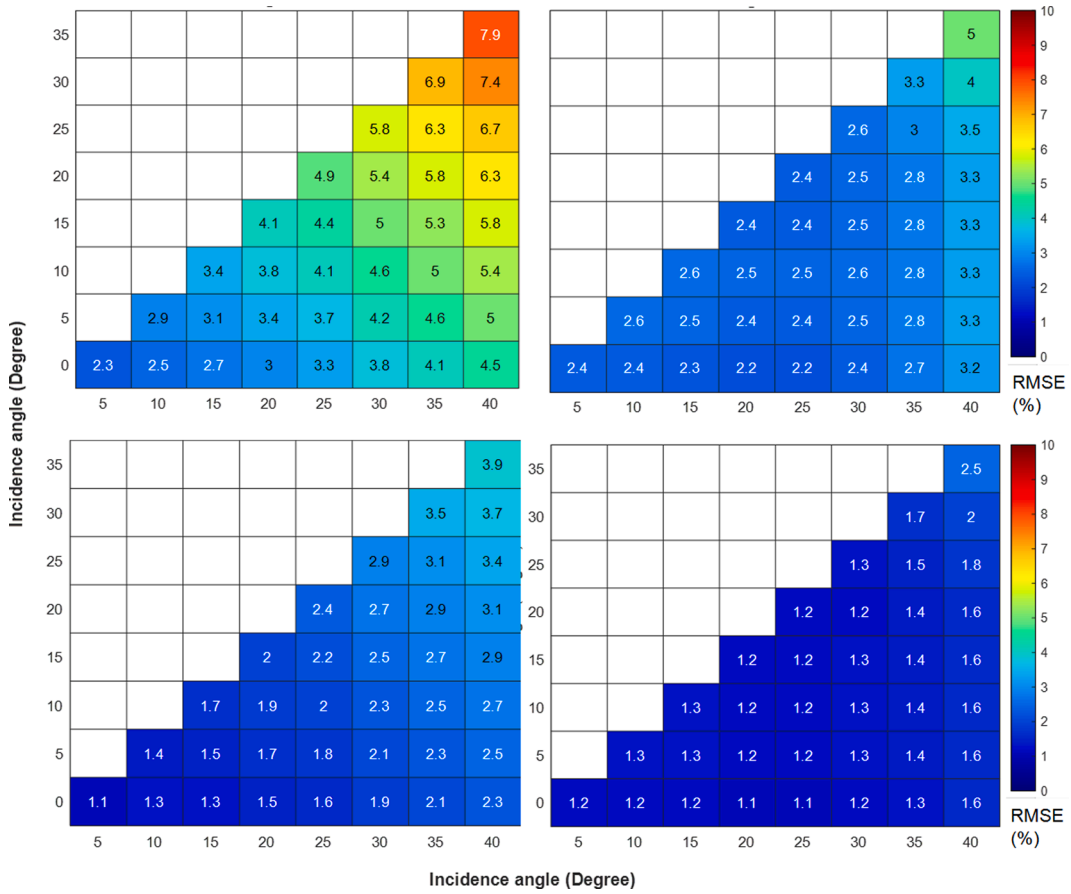

Fig. 15. As for Fig. 14 but for the UGM sub base/base.

carried out and the results from this field test will provide information on the spatial distribution of soil moisture along the corridor.

Conclusion

An L-band radiometer was investigated for measuring SM relative to two different construction materials, sand subgrade and UGM sub base/base. A total of six and four experiments were performed for the sand subgrade and UGM sub base/base material, respectively. The RMSE results in this paper was calculated based on measured data from these repeated experiments, demonstrating the reproducibility and repeatability of this technique. Two approaches to retrieve SM were presented with their achievable accuracy and drawbacks listed. On the basis of the experiments conducted and analysis of data undertaken, the following points can be made:

Using both horizontal and vertical polarization or vertical polarization alone provided better accuracy of SM retrieval than using horizontal polarization for all approaches.

When only one incidence angle was used for SM retrieval, an accuracy of 5 % VMC or 3 % GMC was achieved at angles ranging from 0 to 15° for sand subgrade and 2 % VMC or 1 % GMC at 0° for UGM sub base/base. However, this approach provided very low accuracy at some angles, as low as 13 % VMC or 10 % GMC at 35° for sand subgrade and 4 to 5 % VMC or 2 to 3 % GMC at 35 and 40° for UGM sub base/base, respectively.

Using more incidence angles resulted in slightly improved accuracy of the retrieval results, with the best accuracy of 5 % VMC or 3 % GMC for sand subgrade, but not give better results for UGM sub base/base. In all combination strategies, the combination of smaller incidence angles (0, 5, 10, 15°) provided the highest accuracy, while the combination of larger incidence angles (35 and 40°) resulted in the greatest errors in retrieval results.

The highest accuracy was achieved for both materials when only one incidence angle (at 0°) is used at dual or single (horizontal or vertical) polarization as it is less exposed to the surface roughness effects.

Therefore, using dual or single (horizontal or vertical) polarization alone at 0° is the recommended configuration for use in further field testing when ancillary data such as surface roughness and soil surface temperature is provided. An angle combination consisting of the lowest incidence angle at 0° with another angles (from 5 to 15°) using dual polarization for sand subgrade and vertical polarization alone for UGM sub base/base would be recommended if multi-parameter retrieval approach is used.

The present study focused on finding the best configuration for field testing. In future studies, field trials with the integration of the radiometer into the utility vehicle will be carried out. Specifically, by driving the vehicle along the road construction corridor, microwave brightness temperature (TB) observed from ELBARA at high spatial resolution can be measured. Ancillary measurements (i.e. surface roughness, soil temperature, soil density, and soil texture information) may then be collected or retrieved depending on the retrieval approach. An Inertial Navigation Systems (INS)/Global Positioning System (GPS) can be used to provide information about the geolocation of each measurement point. Accordingly, the SM information and the geolocation of each measurement point can be used to produce a real-time map of soil moisture along the construction corridor.

CRediT authorship contribution statement

Thi Mai Nguyen: Conceptualization, Methodology, Software, Formal analysis, Investigation, Validation, Writing – original draft, Writing – review & editing. **Jeffrey P. Walker:** Conceptualization,

Methodology, Resources, Supervision, Writing – review & editing. **Nan Ye:** Software, Formal analysis. **Jayantha Kodikara:** Resources, Supervision, Funding acquisition, Writing – review & editing.

Declaration of Competing Interest

The authors declare that they have no known competing financial interests or personal relationships that could have appeared to influence the work reported in this paper.

Data availability

The dataset of this paper is available on Mendeley Data: https://data.mendeley.com/datasets/dxmx85m7sw/1.

Acknowledgements

The first author received a Co-Funded Monash Graduate Scholarship (CF-MGS) to undertake this research project. This research work is also part of a research project (Project No IH18.03.2) sponsored by the Smart Pavements Australia Research Collaboration (SPARC) Hub (https://sparchub.org.au) at the Department of Civil Engineering, Monash University, funded by the Australian Research Council (ARC) Industrial Transformation Research Hub (ITRH) Scheme (Project ID: IH180100010). The authors would like to thank the technical staff in the Department of Civil Engineering, Monash University, and fellow PhD students Foad Brakhasi, and Luisa Fernanda White Murillo for their help in supporting the experiment. The ELBARA III was provided by the Institute of Bio- and Geosciences, Forschungszentrum Jülich GmbH, 52425 Jülich, Germany and other equipment were provided by Prof. Jeff Walker's group. The authors would also like to thank the Smart Pavements Australia Research Collaboration (SPARC) Hub, Construction, Infrastructure, Mining and Concessions (CIMIC), and Engineering, Innovation and Capability (EIC) activities for their financial support, and SPARC Hub members for their moral support throughout the experiments.

Funding

This study was supported by the Australian Research Council (ARC) Industrial Transformation Research Hub (ITRH) Scheme (Grant No. IH180100010).

References

[1] Dunham-Friel J, Carraro JAH. Effects of compaction effort, inclusion stiffness, and rubber size on the shear strength and stiffness of expansive Soil-Rubber (ESR) Mixtures. In: Geo-congress 2014: geo-characterization and modeling for sustainability; 2014.
[2] de Carteret R et al. Guide to pavement technology: part 8: pavement construction; 2009.
[3] Mooney MA. Intelligent soil compaction systems. Vol. 676. Transportation Research Board; 2010.
[4] Liu D, Li Z, Lian Z. Compaction quality assessment of earth-rock dam materials using roller-integrated compaction monitoring technology. Autom Constr 2014;44:234–46.
[5] Dunston PS et al. Intelligent compaction of soils—data interpretation and role in QC/QA specifications; 2018.
[6] Ling J, et al. Continuous compaction control technology for granite residual subgrade compaction. J Mater Civ Eng 2018;30(12):04018316.
[7] Salem H. Monitoring and modeling subgrade soil moisture for pavement design and rehabilitation in Idaho Phase III: data collection and analysis; 2004.
[8] Klotzsche A, et al. Measuring soil water content with ground penetrating radar: a decade of progress. Vadose Zone J 2018;17(1):1–9.
[9] Liu X, et al. Measurement of soil water content using ground-penetrating radar: a review of current methods. Int J Digital Earth 2019;12(1):95–118.
[10] Davis JL, Annan AP. Ground-penetrating radar for high-resolution mapping of soil and rock stratigraphy 1. Geophys Prospect 1989;37(5):531–51.
[11] Grote K, et al. Evaluation of infiltration in layered pavements using surface GPR reflection techniques. J Appl Geophys 2005;57(2):129–53.
[12] Shutko AM. Microwave radiometry of lands under natural and artificial moistening. IEEE Trans Geosci Remote Sens 1982;1:18–26.
[13] Kerr YH, et al. Soil moisture retrieval from space: The Soil Moisture and Ocean Salinity (SMOS) mission. IEEE Trans Geosci Remote Sens 2001;39(8):1729–35.
[14] Entekhabi D, et al. The soil moisture active passive (SMAP) mission. Proc IEEE 2010;98(5):704–16.
[15] Ulaby FT, Razani M, Dobson MC. Effects of vegetation cover on the microwave radiometric sensitivity to soil moisture. IEEE Trans Geosci Remote Sens 1983;1:51–61.
[16] Schwank M, et al. ELBARA II, an L-band radiometer system for soil moisture research. Sensors 2010;10(1):584–612.
[17] Kerr YH, et al. The SMOS mission: new tool for monitoring key elements of the global water cycle. Proc IEEE 2010;98(5):666–87.
[18] Emery W, Camps A. Introduction to satellite remote sensing: atmosphere, ocean, land and cryosphere applications. Elsevier; 2017.
[19] Wang J, et al. The L-band PBMR measurements of surface soil moisture in FIFE. IEEE Trans Geosci Remote Sens 1990;28(5):906–14.
[20] O'neill P, Chauhan N, Jackson T. Use of active and passive microwave remote sensing for soil moisture estimation through corn. Int J Remote Sens 1996;17(10):1851–65.
[21] Njoku EG, et al. Observations of soil moisture using a passive and active low-frequency microwave airborne sensor during SGP99. IEEE Trans Geosci Remote Sens 2002;40(12):2659–73.
[22] Bolten J, Lakshmi V, Njoku E. A passive-active retrieval of soil moisture for the Southern Great Plains 1999 Experiment. IEEE Trans Geosci Rem Sens 2003;41:2792–801.
[23] Narayan U, Lakshmi V, Njoku EG. Retrieval of soil moisture from passive and active L/S band sensor (PALS) observations during the Soil Moisture Experiment in 2002 (SMEX02). Remote Sens Environ 2004;92(4):483–96.
[24] Acevo-Herrera R et al. On the use of compact L-band Dicke radiometer (ARIEL) and UAV for soil moisture and salinity map retrieval: 2008/2009 field experiments. In: 2009 IEEE international geoscience and remote sensing symposium. IEEE; 2009.
[25] Acevo-Herrera R, et al. Design and first results of an UAV-borne L-band radiometer for multiple monitoring purposes. Remote Sensing 2010;2(7):1662–79.
[26] Gasiewski A, et al. High resolution UAV-based passive microwave L-band imaging of soil moisture. AGUFM 2013;2013. H31F-1260.
[27] Dai E, et al. High spatial resolution soil moisture mapping using a lobe differencing correlation radiometer on a small unmanned aerial system. IEEE Trans Geosci Remote Sens 2020;59(5):4062–79.
[28] Wah-González CR, Rodríguez-Solís, RA. Design of a low SWaP dual-band radiometer for UAS remote sensing application. In: 2020 IEEE space hardware and radio conference (SHaRC). IEEE; 2020.
[29] Houtz D, Naderpour R, Schwank M. Portable l-band radiometer (polra): design and characterization. Remote Sensing 2020;12(17):2780.
[30] Wu X, et al. Inter-comparison of proximal near-surface soil moisture measurement techniques. IEEE J Sel Top Appl Earth Obs Remote Sens 2022;15:2370–8.
[31] Wigneron J-P, et al. Two-dimensional microwave interferometer retrieval capabilities over land surfaces (SMOS mission). Remote Sens Environ 2000;73(3):270–82.
[32] Zhao T, et al. Refinement of SMOS multiangular brightness temperature toward soil moisture retrieval and its analysis over reference targets. IEEE J Sel Top Appl Earth Obs Remote Sens 2014;8(2):589–603.
[33] Wigneron J-P, et al. L-band microwave emission of the biosphere (L-MEB) model: description and calibration against experimental data sets over crop fields. Remote Sens Environ 2007;107(4):639–55.
[34] Zhao T, et al. Soil moisture retrievals using L-band radiometry from variable angular ground-based and airborne observations. Remote Sens Environ 2020;248:111958.
[35] Guo P, et al. A new algorithm for soil moisture retrieval with L-band radiometer. IEEE J Sel Top Appl Earth Obs Remote Sens 2013;6(3):1147–55.
[36] Al-Yaari A, et al. Evaluating soil moisture retrievals from ESA's SMOS and NASA's SMAP brightness temperature datasets. Remote Sens Environ 2017;193:257–73.
[37] Zheng D, et al. Assessment of soil moisture SMAP retrievals and ELBARA-III measurements in a Tibetan meadow ecosystem. IEEE Geosci Remote Sens Lett 2019;16(9):1407–11.
[38] Fu Y, et al. Soil moisture estimation by combining L-band brightness temperature and vegetation related information. International conference on computer and computing technologies in agriculture. Springer; 2017.
[39] Jamei M, et al. Validation of the SMOS level 1C brightness temperature and level 2 soil moisture data over the west and southwest of Iran. Remote Sensing 2020;12(17):2819.
[40] Ulaby F, Moore R, Fung A. Microwave remote sensing: active and passive. Volume 2-Radar remote sensing and surface scattering and emission theory; 1982.
[41] Al-Yaari AM. Global-scale evaluation of a hydrological variable measured from space: SMOS satellite remote sensing soil moisture products. Université Pierre et Marie Curie-Paris VI; 2014.
[42] Miernecki M, et al. Effects of decimetre-scale surface roughness on L-band brightness temperature of sea ice. Cryosphere 2020;14(2):461–76.
[43] Peischl S. et al. Soil moisture retrieval from multi-incidence angle observations at L-band. In: Proceedings of the 19th international congress on modelling and simulation, Perth, Australia; 2011.
[44] Wigneron J-P, et al. Soil moisture retrievals from biangular L-band passive microwave observations. IEEE Geosci Remote Sens Lett 2004;1(4):277–81.
[45] Saleh K, et al. Semi-empirical regressions at L-band applied to surface soil moisture retrievals over grass. Remote Sens Environ 2006;101(3):415–26.
[46] Mätzler C et al. ELBARA, the ETH L-band radiometer for soil moisture research. In: Proc IGARSS; 2003.

[47] Jing P, Chazallon C. Hydro-mechanical behaviour of an unbound granular base course material used in low traffic pavements. Materials 2020;13(4):852.
[48] Njoku EG, Kong JA. Theory for passive microwave remote sensing of near-surface soil moisture. J Geophys Res 1977;82(20):3108–18.
[49] Pellarin T, et al. Two-year global simulation of L-band brightness temperatures over land. IEEE Trans Geosci Remote Sens 2003;41(9):2135–9.
[50] Le Vine DM, Abraham S. Galactic noise and passive microwave remote sensing from space at L-band. IEEE Trans Geosci Remote Sens 2004;42(1):119–29.
[51] Schmugge T. Measurements of surface soil moisture and temperature. In: Remote sensing of biosphere functioning. Springer; 1990. p. 31–63.
[52] Wang JR, Schmugge TJ. An empirical model for the complex dielectric permittivity of soils as a function of water content. IEEE Trans Geosci Remote Sens 1980;4:288–95.
[53] Dobson MC, et al. Microwave dielectric behavior of wet soil-Part II: dielectric mixing models. IEEE Trans Geosci Remote Sens 1985;1:35–46.
[54] Mironov VL, Kosolapova LG, Fomin SV. Physically and mineralogically based spectroscopic dielectric model for moist soils. IEEE Trans Geosci Remote Sens 2009;47(7):2059–70.
[55] Mironov V, Bobrov P, Fomin S. Dielectric model of moist soils with varying clay content in the 0.04–26.5 GHz frequency range. In: 2013 International Siberian conference on control and communications (SIBCON). IEEE; 2013.
[56] da Silva AP, Kay B, Perfect E. Management versus inherent soil properties effects on bulk density and relative compaction. Soil Tillage Res 1997;44(1–2):81–93.
[57] Mo T, Schmugge TJ. A parameterization of the effect of surface roughness on microwave emission. IEEE Trans Geosci Remote Sens 1987;4:481–6.
[58] Wigneron J-P, Laguerre L, Kerr YH. A simple parameterization of the L-band microwave emission from rough agricultural soils. IEEE Trans Geosci Remote Sens 2001;39(8):1697–707.
[59] Wang J, Choudhury B. Remote sensing of soil moisture content, over bare field at 1.4 GHz frequency. J Geophys Res Oceans 1981;86(C6):5277–82.
[60] Wang JR, et al. Multifrequency measurements of the effects of soil moisture, soil texture, and surface roughness. IEEE Trans Geosci Remote Sens 1983;1:44–51.
[61] Escorihuela MJ, et al. A simple model of the bare soil microwave emission at L-band. IEEE Trans Geosci Remote Sens 2007;45(7):1978–87.
[62] Choudhury B, et al. Effect of surface roughness on the microwave emission from soils. J Geophys Res Oceans 1979;84(C9):5699–706.
[63] Njoku EG, Entekhabi D. Passive microwave remote sensing of soil moisture. J Hydrol 1996;184(1–2):101–29.
[64] Choudhury B, Schmugge T, Mo T. A parameterization of effective soil temperature for microwave emission. J Geophys Res Oceans 1982;87(C2):1301–4.
[65] Wigneron J-P, et al. Estimating the effective soil temperature at L-band as a function of soil properties. IEEE Trans Geosci Remote Sens 2008;46(3):797–807.
[66] Pardé M, et al. N-parameter retrievals from L-band microwave observations acquired over a variety of crop fields. IEEE Trans Geosci Remote Sens 2004;42(6):1168–78.